A Case Study of the Sensitivity of Numerical Simulation of Mesoscale Convective Systems to Varying Initial Conditions

DA-LIN ZHANG* AND J. MICHAEL FRITSCH

Department of Meteorology, The Pennsylvania State University, University Park, PA 16802

(Manuscript received 18 March 1986, in final form 19 May 1986)

ABSTRACT

A 12 h nested-grid numerical simulation of a warm-season mesoscale convective weather system (Zhang and Fritsch, 1986) is utilized as a control run in order to 1) test the sensitivity of the numerical simulation to different types of initial conditions; 2) examine the need for an observing system that would resolve mesoscale features; and 3) determine which meteorological variables need to be most carefully considered in observing system design and preprocessing analysis.

It is found that improved observational capabilities are likely to have an important impact on the successful prediction of the timing and location of summertime mesoscale convective weather systems if mesoscale features can be resolved. In particular, the resolution of the moisture field significantly affects the prediction of the evolution of the convective weather systems. Correspondingly, the mesoscale distribution of precipitation is substantially affected, especially the location of the areas of heavy rain. It is also found that procedures to account for the effects of convective systems that are in progress at the time of initialization can make significant contributions to the prediction of the evolution of the meteorological events and to the improvement of the quantitative precipitation forecasts. In particular, in weak-gradient summertime situations, mesoscale convective systems can severely alter their near environment within a short time period by producing strong mesoscale circulations, thermal boundaries, moist adiabatic stratifications, etc.

For summertime situations where the large-scale gradients are weak, detailed temperature and moisture fields appear to be more important than the detailed wind fields in determining the development and evolution of deep convection. However, poor resolution of the wind field such that wind speed magnitudes and gradients are underestimated tends to reduce the degree of mesoscale organization. It also alters the magnitude and distribution of low-level convergence, and this affects the evolution of the thermodynamic fields and the deep convection.

Incorporation of dense surface observations into the initial conditions can be very important in improving forecasts of meso-β-scale structures such as moist (dry) tongues, thermal boundaries, and, in particular, pressure distribution. Most significantly, the large (meso-α)-scale environment appears to contain some type of signal such that the *general* evolution of events is similar, even when the initial mesoscale structure and the simulated meso-β-scale evolution of events are significantly different. On the other hand, poor resolution of meso-α-scale gradients can substantially alter the predicted evolution of meso-β-scale features and the location of heavy rain.

1. Introduction

Since the advent of numerical weather prediction in the 1950s, skill in predicting the daily weather has increased considerably (Fawcett, 1977; Shuman, 1978; Charba and Klein, 1980; Glahn, 1985). Increases in model skill are, to a large extent, dependent upon improvements in four factors: 1) numerical techniques; 2) model physics; 3) computer power; and 4) initial conditions. Of these four, the first three have progressed fairly rapidly for small- to large-scale models while, on the other hand, progress in obtaining better initial conditions (especially for meso-α or smaller scales) has been slow. This is almost paradoxical since there have been great strides in observational technology during the past three decades (see Gage and Green, 1982; Hogg et al., 1983; Westwater et al., 1985). The difficulty seems to be that each new observing system has one or more of the following problems: 1) data are generated in a form not readily usable in numerical models; 2) vertical resolution is inadequate; 3) data are not always available; and 4) the observing system only covers a fraction of the required area (usually because it is prohibitively expensive to establish a dense network). Nevertheless, as numerical models become more sophisticated, evidence continues to mount that a substantial improvement in forecasting skill would result if better initial data were available (see Perkey, 1976; Kelly et al., 1978; Anthes et al., 1981; Carpenter and Lowther, 1982; Chang et al., 1984). Moreover, a number of simulations of observing systems have indicated that numerical models are very sensitive to changes in initial temperature, moisture, and horizontal winds (Kelly et al., 1978; Perkey, 1976; Chang et al., 1984).

The objectives of this paper are to 1) test the sensi-

---

* Present Affiliation: National Center for Atmospheric Research, Boulder, CO 80307.

tivity of a numerical simulation of mesoscale convective systems (MCSs) to different types of initial conditions; 2) examine the need for a high resolution observing system that is compatible with the scale of the model simulation; and 3) determine which meteorological variables need to be most carefully considered in observing-system design and preprocessing analysis. The experiments presented here use an 18-h simulation of the 1977 Johnstown flood (see Zhang, 1985; Zhang and Fritsch, 1986) as a control run to investigate the impact of different initial data on the simulation of the MCSs. Section 2 briefly presents the basic features in the model and describes the control simulation. Section 3 provides the experimental design with different initial conditions. Sensitivities of the model response to the different initial conditions are examined in section 4. A summary and concluding remarks are given in the last section.

2. Model description and control simulation

A modified version of the PSU/NCAR[1] mesoscale model originally developed by Anthes and Warner (1978) was used for this study. The following changes/additions were introduced:

- a two-way interactive nested-grid procedure (Zhang et al., 1986);
- a modified version of the Fritsch–Chappell (1980) convective parameterization for the fine-mesh portions of the nested-grid model (Zhang and Fritsch, 1986);
- an R. A. Anthes–H. L. Kuo type of convective scheme for the coarse-mesh portions of the nested-grid model (Anthes and Keyser, 1979);
- a modified version of the Blackadar "large-eddy exchange" boundary-layer parameterization (Zhang and Anthes, 1982; Zhang and Fritsch, 1986);
- a porous sponge, lateral-boundary condition (Perkey and Kreitzberg, 1976) for the outermost coarse-mesh boundary; and
- virtual temperature effects in the gas law.

The nested-grid ratio is 1 to 3 with a fine-mesh length of 25 km and a coarse-mesh length of 75 km. The (x, y, σ) dimensions of the coarse and fine meshes are 39 $\times$ 31 $\times$ 19 and 43 $\times$ 37 $\times$ 19, respectively. Figure 1 shows the nested-grid domains for the study. Since the results from the fine-mesh domain are of greater interest, the following discussions will be confined to the fine-mesh output. For more details of the model, the reader is referred to Zhang (1985) and Zhang and Fritsch (1986).

The Johnstown flood of July 1977 was produced by a combination of heavy rainfalls from a squall line and a mesoscale convective complex (MCC). In general, the control simulation reproduced the size, propagation rate, and orientation of the squall line and MCC fairly well. The simulated evolution of other meteorological features, such as the diurnal boundary layer, cool outflow boundaries, low-level jet, and surface pressure perturbations, (e.g., meso-β-scale lows, highs, ridges, and troughs), compare favorably to observational analyses by Hoxit et al. (1978) and Bosart and Sanders (1981). It is of particular significance that the model-predicted rainfall distribution and magnitude are similar to the observed one. (See Zhang and Fritsch, 1986, for a comparison of the observed and simulated evolution of events.) Figure 2 shows only a portion of the evolution of the surface features from the control simulations (Exp. CTS). These few figures are considered to be sufficient as a basis for comparisons with sensitivity experiments described in the next two sections. Note that the area of deep convection initially over Lake Erie (Fig. 2a) elongates into a NE–SW oriented squall line (Fig. 2b) and propagates eastward across Pennsylvania. By 1800 GMT (Fig. 2c), the squall line has intensified and separated from the original convective system (hereafter termed pre-MCC) still located over northwestern Pennsylvania. Note also that a distinct mesolow has developed in the same region as the pre-MCC. At 0000 GMT (Fig. 2e), only the northeastern portion of the squall line remains active. The mesolow and pre-MCC also propagate eastward as yet a third region of deep convection develops over western Pennsylvania. The simulated 12-h accumulated precipitation is shown in Fig. 2f. Note that the orientation of maximum rainfall over northwestern Pennsylvania corresponds to the path of the mesolow. As pointed out in Zhang and Fritsch (1985; 1986), grid-resolvable

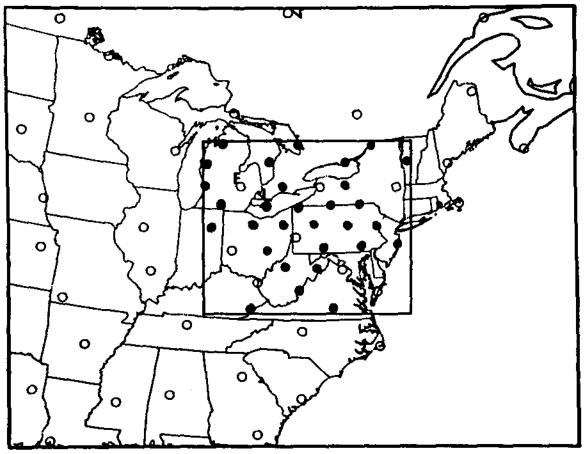

FIG. 1. Nested-grid domain with distribution of standard rawinsonde stations and the Bosart sounding locations. The interior thick solid lines denote the mesh interface. The open circles are the location of standard rawinsonde stations while the solid circles are the Bosart sounding locations. Symbols F and L denote the locations of the Flint, Michigan and Lake Erie soundings, respectively.

---

[1] PSU/NCAR: The Pennsylvania State University/National Center for Atmospheric Research, which is sponsored by the National Science Foundation.

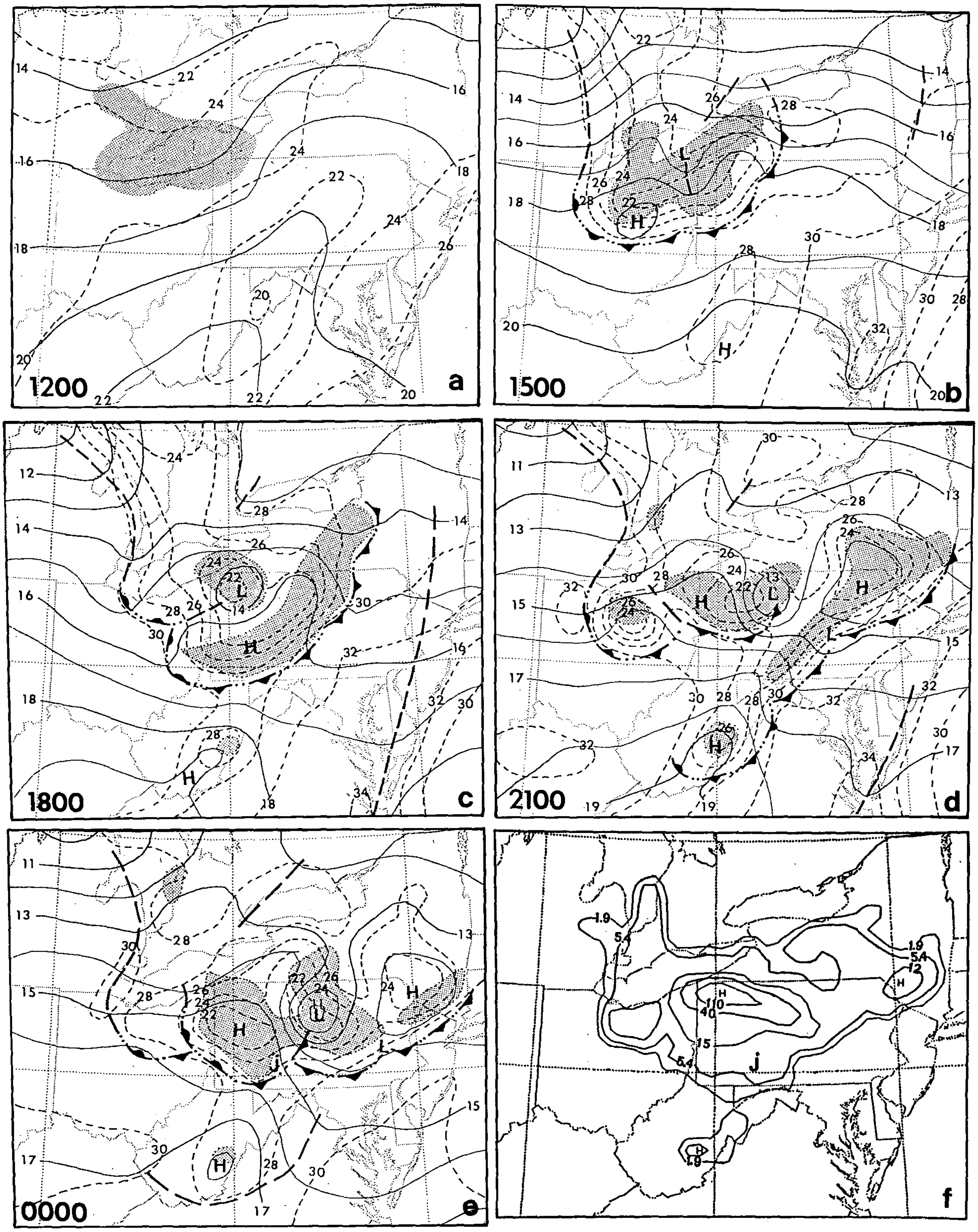

FIG. 2. (a)–(e) Analysis of sea level pressure (solid line, mb) and surface temperature (dashed line, °C) for the times indicated. Shading denotes the area of active convection produced by the convective parameterization scheme. Heavy dashed lines indicate troughs; frontal symbols alternated with double dots denote cool outflow boundaries. (f) Predicted 12 h accumulated rainfall (mm) for the period 1200 GMT 19 July to 0000 GMT 20 July 1977.

scale condensation made a significant contribution to the total rainfall (30–40%).

Although the control simulation is encouraging when compared with observations, the meso-β-scale details critically depend upon the introduction of soundings from a subjective mesoanalysis by Lance Bosart (personal communication, 1982). Specifically, Bosart produced a 1° latitude–longitude resolution, three-dimensional analysis of temperature, dewpoint, and horizontal winds that helps define mesoscale features. In addition to eight conventional rawinsonde observations in the fine-mesh domain, thirty "soundings" were selected from the Bosart analysis to aid in resolving mesoscale structure. (See Fig. 1 for the distribution of sounding locations.) Sections 3 and 4 provide discussions of the model's sensitivity to these additional soundings.

3. Experimental design

In order to assess the effect of varying initial conditions on the simulation of the MCSs, the following six different initial data sets were used for sensitivity experiments:

(a) Only regular rawinsonde observations (i.e., no Bosart soundings; Exp. NBS). The objective of this experiment is to evaluate the significance of introducing mesoscale sounding information. Figure 3 shows the initial 500 mb height and thermal fields for Exps. NBS, NTQ (defined in subsection 3d), and the control case. Note that when the "mesoscale" soundings are omitted (Fig. 3b), the flow becomes more cyclonic over Michigan and nearly zonal across Pennsylvania and New York. Note also that the wedge of warm air over the Great Lakes extends farther west than in the control run, and a closed low appears over eastern Michigan.

(b) The standard soundings plus one Bosart sounding over Lake Erie (Exp. OBS; see Fig. 4a). The objective of this experiment is to crudely examine the effect of the convective system that was in progress at the time of initialization. Specifically, at the time of initialization, satellite imagery shows a significant area of convective clouds over the Lake Erie region (see Zhang and Fritsch, 1986) whereas there is not available observations to represent the atmospheric conditions within the developing convective system. (See Fig. 1 for sounding locations.) The Bosart Lake Erie sounding was primarily determined using satellite information, surface and ship observations, prior soundings, and the standard sounding at Flint, Michigan (see Fig. 4b). Note in Fig. 4a the near-saturated and near-moist-adiabatic thermodynamic conditions over Lake Erie. This presumably resulted from repeated convective overturning and mesoscale ascent during the 4-day period when the MCS propagated from South Dakota toward Pennsylvania (see Bosart and Sanders, 1981). Note also the strong *low-level* westerly winds. The 500 mb height and thermal fields are not shown for this case because,

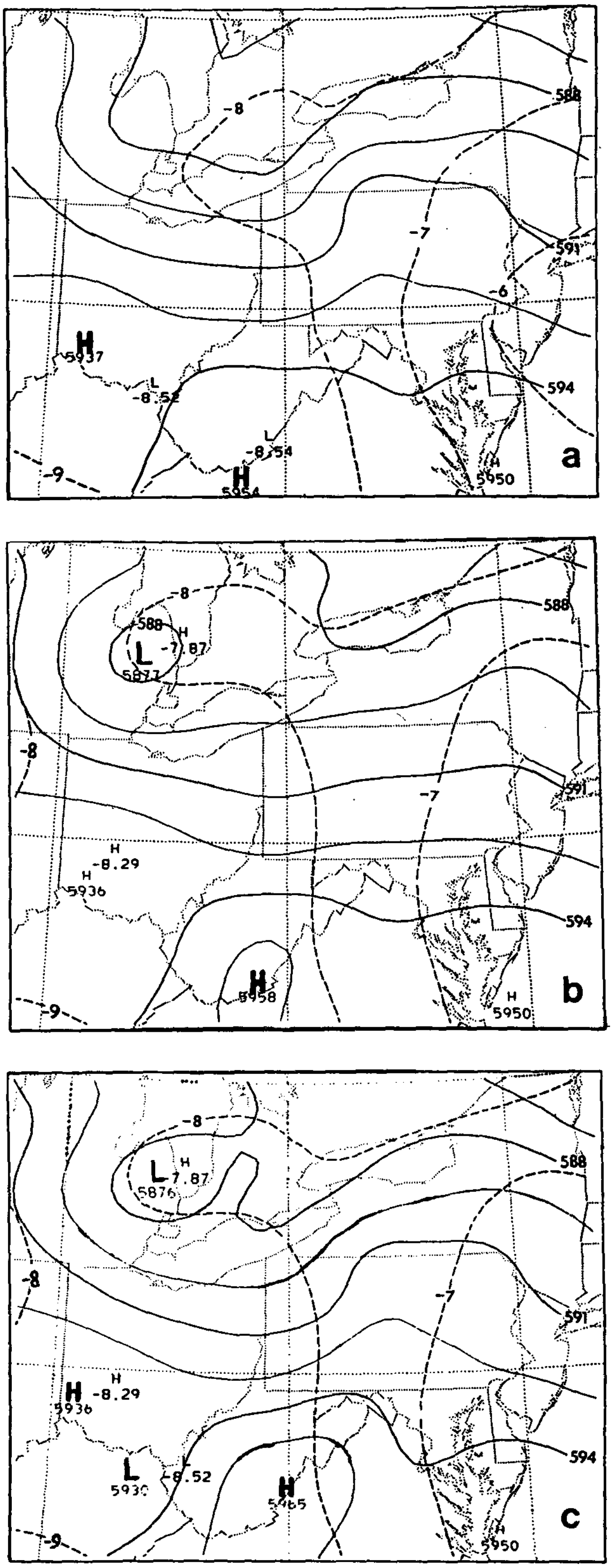

FIG. 3. Comparison of initial height and temperature distributions at 500 mb for (a) Exp. CTS, (b) Exp. NBS, and (c) Exp. NTQ. Solid lines denote heights (dam) and dashed lines indicate temperature (°C).

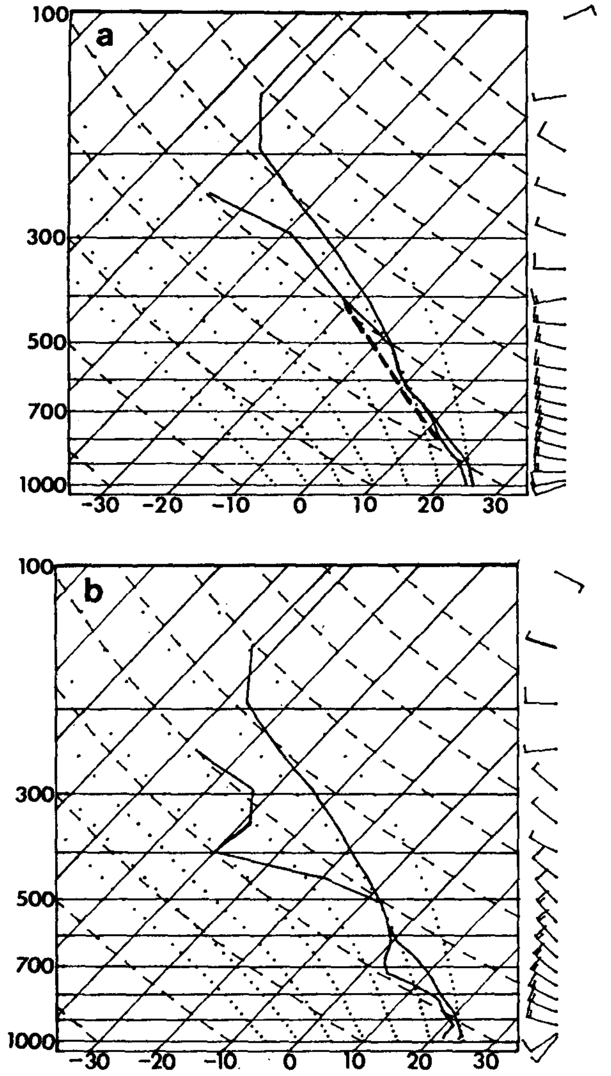

FIG. 4. (a) The Bosart sounding over Lake Erie, and (b) the observed sounding at Flint, Michigan. The heavy dashed line in (a) is the modified moisture profile for Exp. OBO. A full wind barb is 10 m s^{-1} and the direction convention is standard.

as would be expected, they are very similar to Exp. NBS.

(c) Initial conditions identical to the control run except that specific humidity in the Lake Erie sounding is artifically reduced in the 850–500 mb layer (Exp. OBO; see Fig. 4a). Thus, the near-saturated condition is no longer present over the Lake Erie region. The objective is to test the importance of a near-saturated condition in producing the Johnstown flood event and determine the impact of a "bad observation" in the moisture field.

(d) Omitting all the Bosart temperature and moisture information from the Bosart soundings while holding all other initial conditions the same as in the control run (Exp. NTQ). Note that while only the Bosart wind information is added in the model initialization, the dense surface observations were included in the preprocessing procedure to derive grid point surface pressure (see Zhang, 1985 for details). Thus, the surface pressure field is the same as in the control case. The objective of this experiment and the following one is to test the hypothesis that the thermodynamic structure dominates the evolution of summertime MCSs which develop within benign meteorological environments. In other words, when the mesoscale or synoptic-scale dynamic forcing is weak, but generally favorable for the initiation of convection, the evolution of convective activity most strongly depends upon 1) the preexisting large-scale thermodynamic structure of the environment, and 2) the changes in that environment from latent heating and sensible heat redistribution by the convection. Figure 3c shows the 500 mb height field for Exp. NTQ. The observed height pattern over the Great Lakes region is poorly represented while over other regions it is similar to the control conditions. The similarity of the height field between Exps. NTQ and CTS is due to the fact that the same surface pressure field was utilized to derive the geopotential height.

(e) Identical initial conditions to the control run except that the wind information from all Bosart soundings and the Flint, Michigan sounding is excluded (Exp. NUV). Figure 5 shows the initial 900 mb wind field with and without the Flint, Michigan and mesoscale (Bosart) wind information. The Flint sounding is omitted because, like the Bosart sounding over Lake Erie, it contained a strong low-level wind maximum. Note that this wind maximum is associated with the existence of a cool pool to the north via thermal wind considerations (see Zhang and Fritsch, 1986). When only the Bosart wind information is omitted, there is little change in the initial magnitude and location of the low-level jet and associated area of low-level convergence. However, the omission of the Flint *and* Bosart wind information causes a substantial weakening and southward shift of the low-level jet that was over Michigan and the eastern Great Lakes. Such a southward shift of the low-level jet is a little inconsistent with the mass field in this region. Nevertheless, this is considered to be a meaningful test of the impact of losing a key piece of wind data that is crucial for defining a mesoscale feature in the initial conditions. Thus the experiment is designed in the same sense as Exp. NTQ; i.e., to investigate the relative importance of mesoscale wind information vs the significance of detailed thermodynamic structure.

(f) The National Meteorological Center (NMC) global analysis of sea level pressure is directly utilized to obtain grid point surface pressure values without any enhancement from dense surface observations (Exp. PNM). Figure 6 shows the NMC sea level pressure and 500 mb height fields at the initial time. Note the relatively flat sea level pressure perturbation and weak meso-α-scale short wave trough at 500 mb in compar-

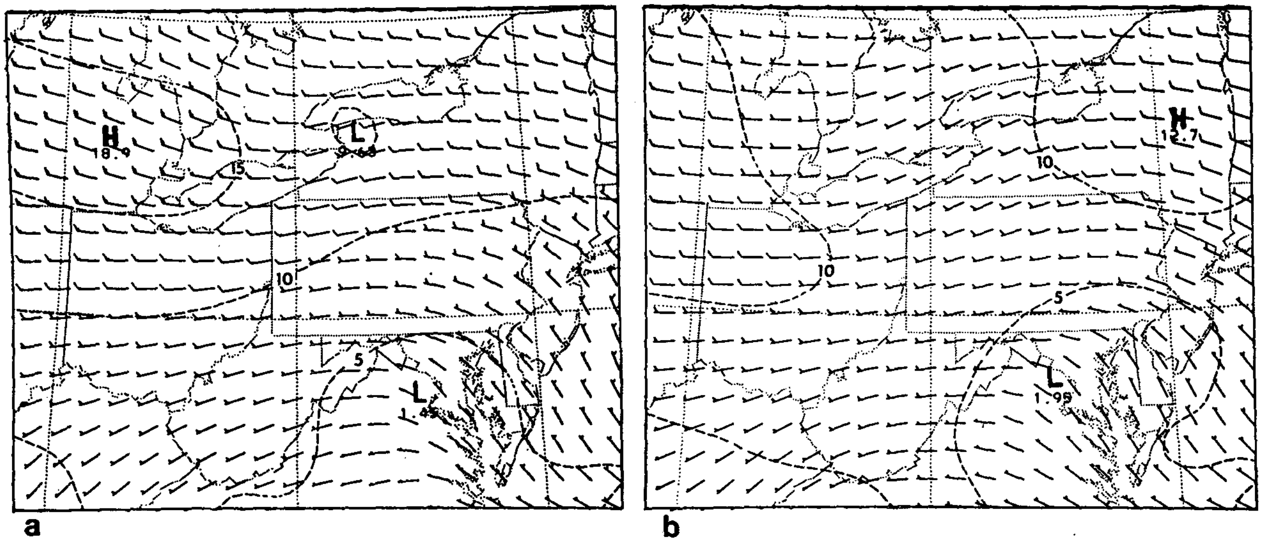

FIG. 5. Analysis of 900-mb wind field (m s^{-1}) at 1200 GMT 19 July 1977 for (a) Exp. CTS and (b) Exp. NUV. A full barb is 10 m s^{-1}.

ison with the control run (see Figs. 2a and 3a). To reduce any strong ageostrophic wind components for such a smoothed wave structure, the wind is assumed to be geostrophic at and above 700 mb. At the surface, observed winds are utilized. Between 700 mb and the surface level, linearly interpolated winds between the geostrophic value and the observed value at individual levels are used. Thus, this set of initial conditions should significantly reduce the forcing from the meso-α scale short wave. Since the observational studies by Hoxit et al. (1978) and Bosart and Sanders (1981) emphasize the role of the meso-α-scale short wave in initiating and organizing the MCSs in the Johnstown flood case, this test should give some indication of the effect of the initial meso-α-scale pressure wave on the development of the MCSs over the Great Lakes region. Note that changing initial conditions in Exps. NBS, OBS, and NTQ also altered the distribution of the short wave perturbation, as mentioned before, but did not weaken the wave to the degree imposed in this experiment.

As will be shown in section 4, the results from each of these experiments have different implications with regard to the improvement of the model forecast skill and to understanding the relative importance of incorporating different data.

4. Results

The effects of varying the initial conditions are evaluated through comparisons of different horizontally mapped fields with those from the control simulation. Specifically, the impact of changing initial conditions is assessed within the context of total rainfall distribution, the evolution of convective activity, surface pressure perturbations, and outflow boundaries. These variables are found to be the best indicators of the model's sensitivity and to have the most practical significance from a user standpoint. Moreover, it was noted during the experimentation that after 12 hours of simulation, clear differences were readily apparent for changes in the initial conditions. Thus, a 12 h model run for each experiment is considered to be sufficient for comparison purposes. Table 1 lists the central pressure of the major mesolow along with the total convective and resolvable-scale rainfalls for each of the experiments. It is apparent that the development of the mesolow is strongly correlated with the resolvable-scale precipitation. Figures 7 and 8 show the 6 and 12 h distributions, respectively, of model convection, surface pressure systems, and outflow boundaries for individual experiments. Figure 9 presents the corresponding 12 h rainfall distributions. Note that *for most of the experiments, the general evolution of events is similar.* Specifically, a line of convection propagates eastward, then weakens, and is followed by a convective redevelopment over the western flank of the cool moist downdraft air from the previous convection. This implies that *all of the different initial conditions contain an important large (meso-α)-scale signal capable of generating the same basic features.* On the other hand, there were significant differences in the timing, location, and intensity of the meso-β-scale features, especially the major mesolow. The specific sensitivities are given as follows.

a. Initial convective distribution

In the model, the area of initial convection is largely determined by the combination of a conditionally unstable stratification and low-level convergence (see Fritsch and Chappell, 1980; Zhang and Fritsch, 1986). Without any of Bosart's thermodynamic information (Exps. NBS and NTQ), the area of initial model con-

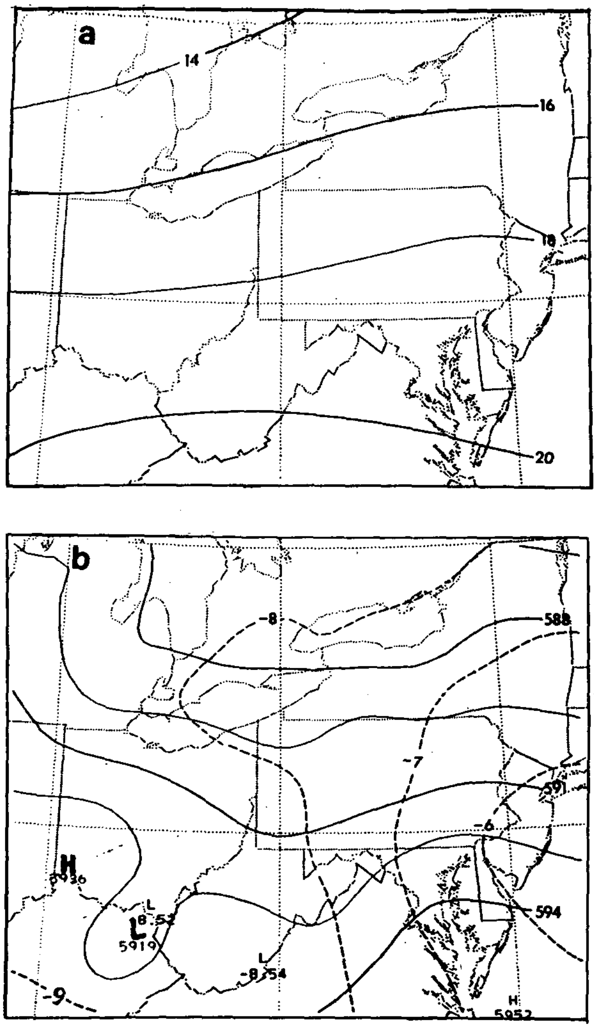

FIG. 6. (a) Sea-level pressure (mb) and (b) 500 mb height (solid line, dam) and temperature (dashed line, °C) at 1200 GMT 19 July 1977 for Exp. PNM.

vection is generated over eastern Michigan and southwestern Ontario (see Figs. 7a, d) instead of over Lake Erie where it actually developed (see Hoxit et al., 1978; or Zhang and Fritsch, 1986). By adding just the Lake Erie sounding (Exp. OBS; see Fig. 7b), the model is able to more closely predict the observed area of initial development of deep convection. Moreover, note that even after the low-level wind field is substantially altered (Exp. NUV; see Fig. 5), the deep convection still develops over Lake Erie (see Fig. 7e) if the thermodynamic information is left unchanged. The initial location of deep convection for Exps. OBO and PNM is also close to the control case (see Figs. 7c and f).

b. Six h simulations

After six hours, both the observations and the control simulation indicate that the squall line separates from the pre-MCC over northwestern Pennsylvania and a mesolow develops in association with the pre-MCC. The numerical solution most similar to this scenario is from Exp. NUV. In this experiment, the Flint wind information and all of Bosart's wind information is removed from the initial conditions. Although the model generates features similar to the control run (see Figs. 2c and 7e), the convective configuration and pressure perturbations in Exp. NUV are not as well organized. Note also that the cooling by moist downdrafts is weaker and the area of convection over West Virginia is considerably larger. Thus, changes in the low-level wind maximum interact with the thermodynamic fields and with the convective parameterization to alter the organization and evolution of the deep convection.

Removing all of Bosart's *thermodynamic* information (Exp. NTQ; see Fig. 7d) from the initial conditions produces some of the most significant differences. In particular, the model fails to produce the major mesolow and associated convection, and the squall line extends too far to the south. The latter error is probably due to the omission of the dry tongue that appeared across West Virginia and south central Pennsylvania in the Bosart analysis.

When all of Bosart's soundings are omitted, the evolution of the convection is similar to that when just the temperature and humidity information is removed and the wind information is retained (see Figs. 7a, d). Note, though, that the distribution of cooling by moist downdrafts is different in these two runs. This probably

TABLE 1. Predicted 12-h accumulated total convective (V_c) and resolvable-scale (V_r) rainfall volume and minimum sea-level pressure (P_m) of the mesolow for different sensitivity experiments. Omission of a sea-level pressure value indicates that the major mesolow did not develop.

Code	Description of experiment	V_c (10^{12} kg)	V_r (10^{12} kg)	P_m (mb)
CTS	Control simulation	2.24	1.77	1011
a: NBS	No mesoscale (Bosart) soundings	2.72	0.27	1013
b: OBS	One mesoscale (Bosart) sounding	3.31	1.56	1009
c: OBO	One "bad" sounding	2.15	0.06	—
d: NTQ	No temperature and moisture information from the Bosart soundings	3.27	0.05	—
e: NUV	Wind information removed from the Bosart and Flint, Michigan soundings	2.25	1.37	1011
f: PNM	Weakened meso-α-scale short wave	3.40	0.11	—

reflects the different distributions of vertical wind shear in the two experiments since the amount of moist downdraft air in the Fritsch–Chappell convective parameterization scheme is strongly affected by vertical wind shear. Note that in both Figs. 7a, d there is a weak low over Lake Erie. This low eventually becomes a weak mesovortex in Exp. NBS (Fig. 7a) while in expt NTQ (Fig. 7d) it does not.

Adding just the Lake Erie sounding into the initial conditions (Exp. OBS; Fig. 7b) does not make much of an improvement in the distribution of convective activity (see Figs. 7a, b, and 2c). However, two significant changes are apparent; specifically, a strong outflow boundary is generated ahead of and behind the major convective system over Pennsylvania and a new mesolow is evident along the Pennsylvania–New York border. This mesolow is apparently an analogous feature to the main mesolow in the control simulation. Note, though, that the mesolow propagates along a path slightly to the north of and has a higher central pressure than that in the control run (see Figs. 7b and 2c). More insight into the importance of the Lake Erie sounding can be gained by comparing Exp. OBS to Exp. OBO (Figs. 7b, c). Surprisingly, in Exp. OBO (Fig. 7c) the model only duplicated the propagation of the squall line, but completely failed in generating the mesolow. These two experiments plus the control simulation clearly indicate that the near-saturated conditions in low- to midlevels have an important contribution to the vortex generation. Note that in place of the mesolow in Exp. OBO, a strong mesohigh dominates all of western Pennsylvania. The pool of cool downdraft air is more extensive and the temperature gradient behind the squall line is stronger than that in the control run. Several other experiments have been conducted to test the importance of incorporating other Bosart soundings into the model initial conditions. The results (not shown) indicate that the Bosart data over central Ohio and central Pennsylvania also have a significant effect on the simulation of the convective systems.

Finally, the effect of weakening the meso-α-scale short wave is considered (Exp. PNM; Fig. 7f). After 6 h of simulation, the deep convection has spread out much farther than in any of the other experimental simulations. This suggests that the convection itself and the resulting mesoscale circulations and outflow boundaries are playing a more significant role in determining the evolution of further convection than the meso-α-scale short wave. Thus, the structure and evolution of mesoscale convective weather systems that develop in the dynamically weak environments of summertime apparently depend upon a complicated interplay of environmental forcing, the characteristics of the convection, and the mesoscale circulations that develop in response to the convection. This sensitivity was originally noted in numerical experiments by Fritsch and Chappell (1981). It is also important to note here that the major mesolow over northwestern Pennsylvania failed to develop in this simulation even though all the Bosart soundings were included in the initial conditions (see Figs. 7f and 8f). Thus, it appears that *the convectively generated low- to midlevel near-saturated environment is only a necessary condition for the generation of the mesovortex. The larger-scale forcing plays an important role in centralizing upward motion so that the positive feedback among latent heat release, low-level moisture convergence, and surface pressure falls can be triggered.*

c. Twelve h simulations

At 0000 GMT, both observations and the control simulation show that the MCC was intensifying over western Pennsylvania while the squall line was dissipating as it propagated into the eastern part of the state (see Hoxit et al., 1978; Zhang and Fritsch, 1986). In general, all of the sensitivity simulations exhibit various degrees of error in predicting the timing, location, and intensity of these meso-β-scale events (see Figs. 8 and 2). Except for Exp. OBO (in which the model was unable to reproduce the widespread convection over western and central Pennsylvania), one of the most common errors is that the area of convective activity is too widespread and extends too far to the west. Also, the strength of the major mesohighs and mesolows varies considerably. On the other hand, the location of the eastern and western outflow boundaries is reasonably consistent from one simulation to another. The loss of thermodynamic information seems to have the most effect on the solution (e.g., see Figs. 2, 8d, e) although the weakening of the short wave (Exp. PNM; Fig. 8f) also results in significant departures from the control run. The 12 h forecast most similar to the control simulation (and the observed conditions) is still Exp. NUV, although there is a significant error in the location of deep convection over Ohio (see Figs. 2e and 8e). The southward shift of the weak, low-level convergence from the Lakes region to central Ohio was unable to trigger deep convection over Ohio during the first 6 h of the simulation. Apparently though, the cumulative effects of the changes in the wind field were such that the environment became more favorable for deep convection over Ohio in the second six hours of the simulation. New convection repeatedly developed along the western flank of the moist downdraft outflow boundary and propagated westward into central Ohio.

Only when the short wave is significantly damped (Exp. PNM; Fig. 8f) or when the thermodynamic information is altered in the key region of convective development (Exps. NBS, OBO, and NTQ; Figs. 8a, c, d, respectively) does the meso-β scale solution show substantial departures from the control run. Thus, *in this case,* the reproduction of the meso-β-scale evolution of events appears to hinge on resolving both the mesoscale thermodynamic structure and the mesoscale forcing (dynamics) in the initial conditions.

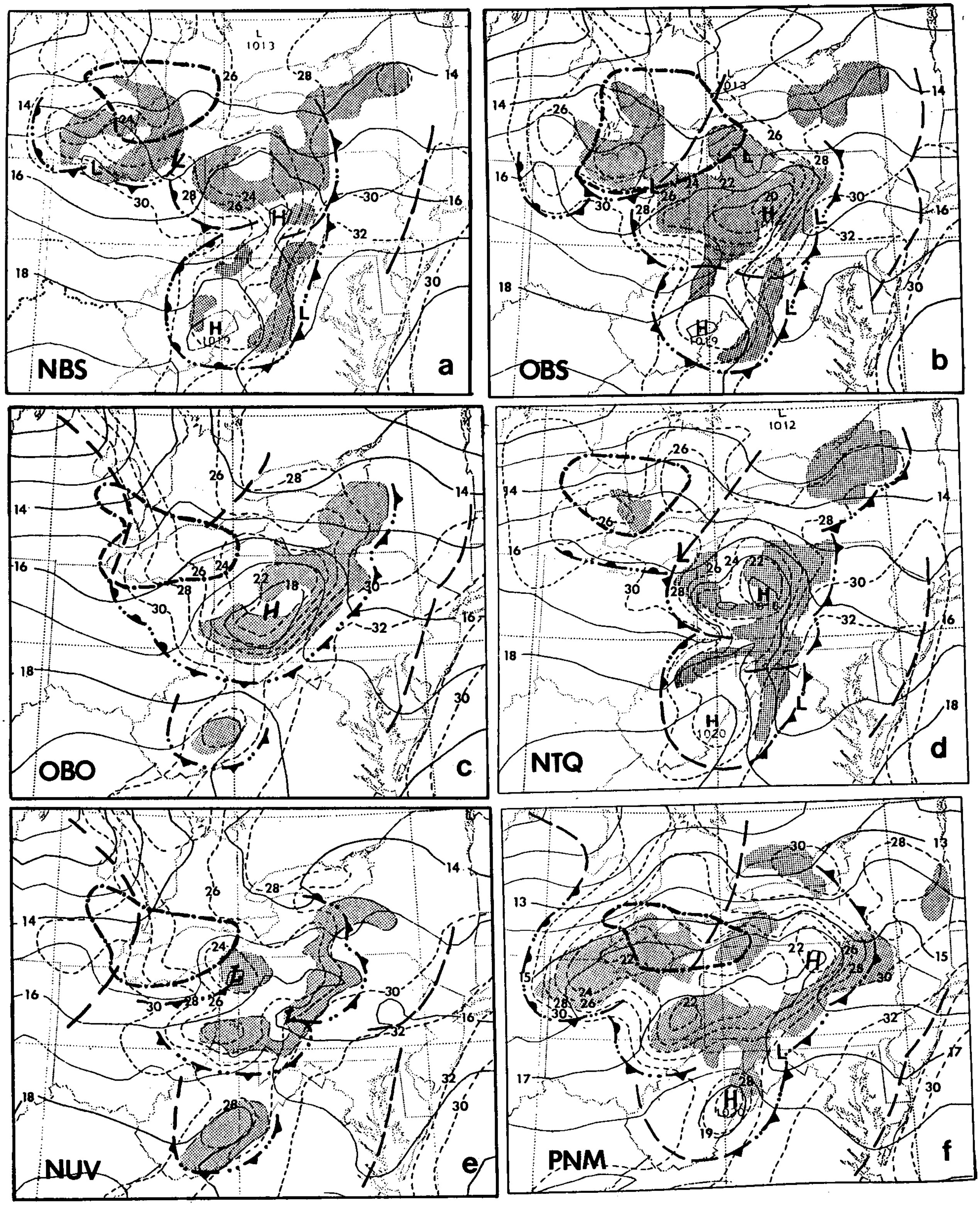

FIG. 7. Analysis of predicted 6 h sea-level pressure (solid line, mb) and surface temperature (dashed lines, °C) for expts (a) NBS, (b) OBS, (c) OBO, (d) NTQ, (e) NUV, and (f) PNM. Thick dot–dashed lines denote initial area of convection. Heavy dashed lines indicate troughs; frontal symbols alternated with double dots denote outflow boundaries. Shading indicates area of active convection.

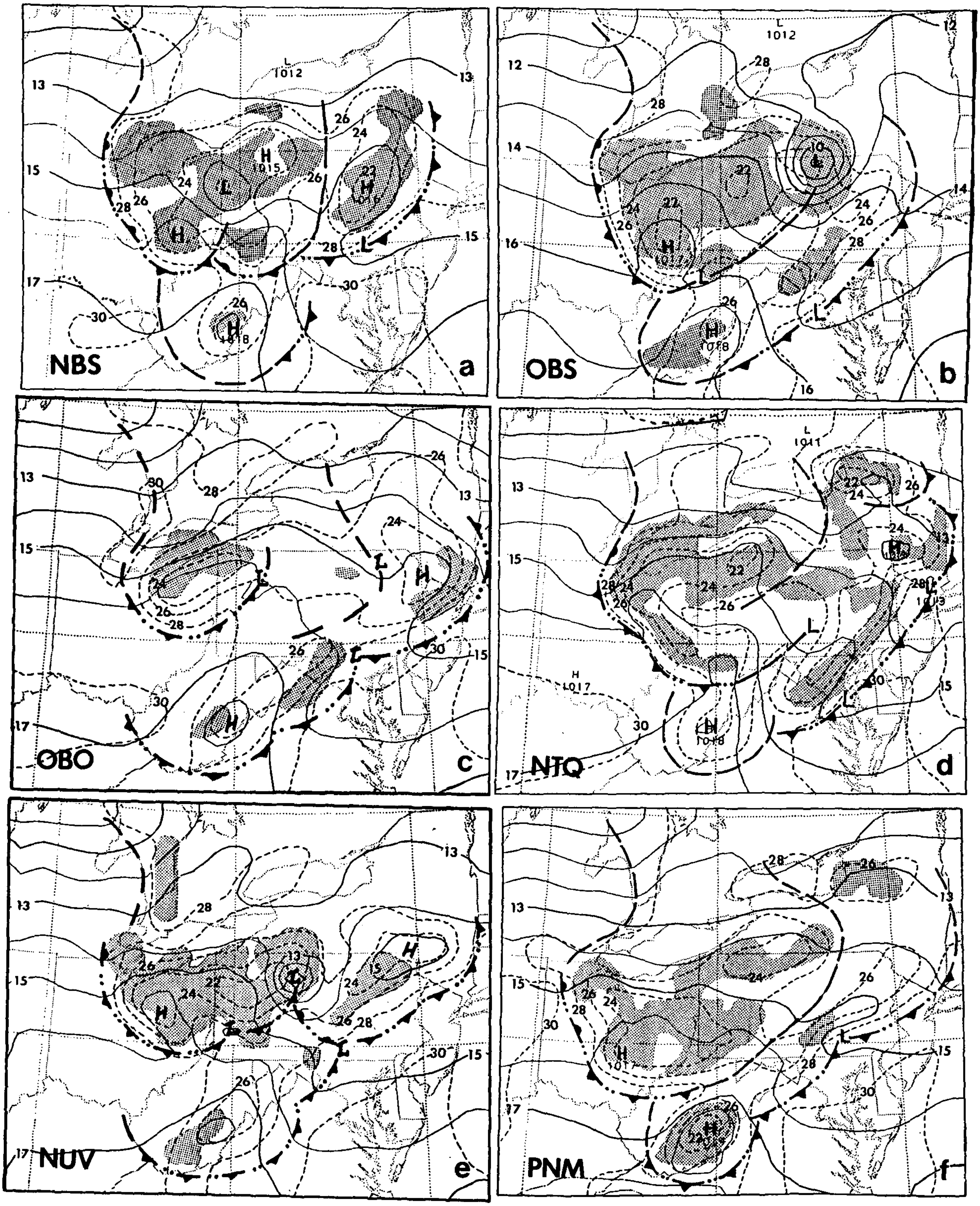

FIG. 8. As in Fig. 7 except for 12 h forecast.

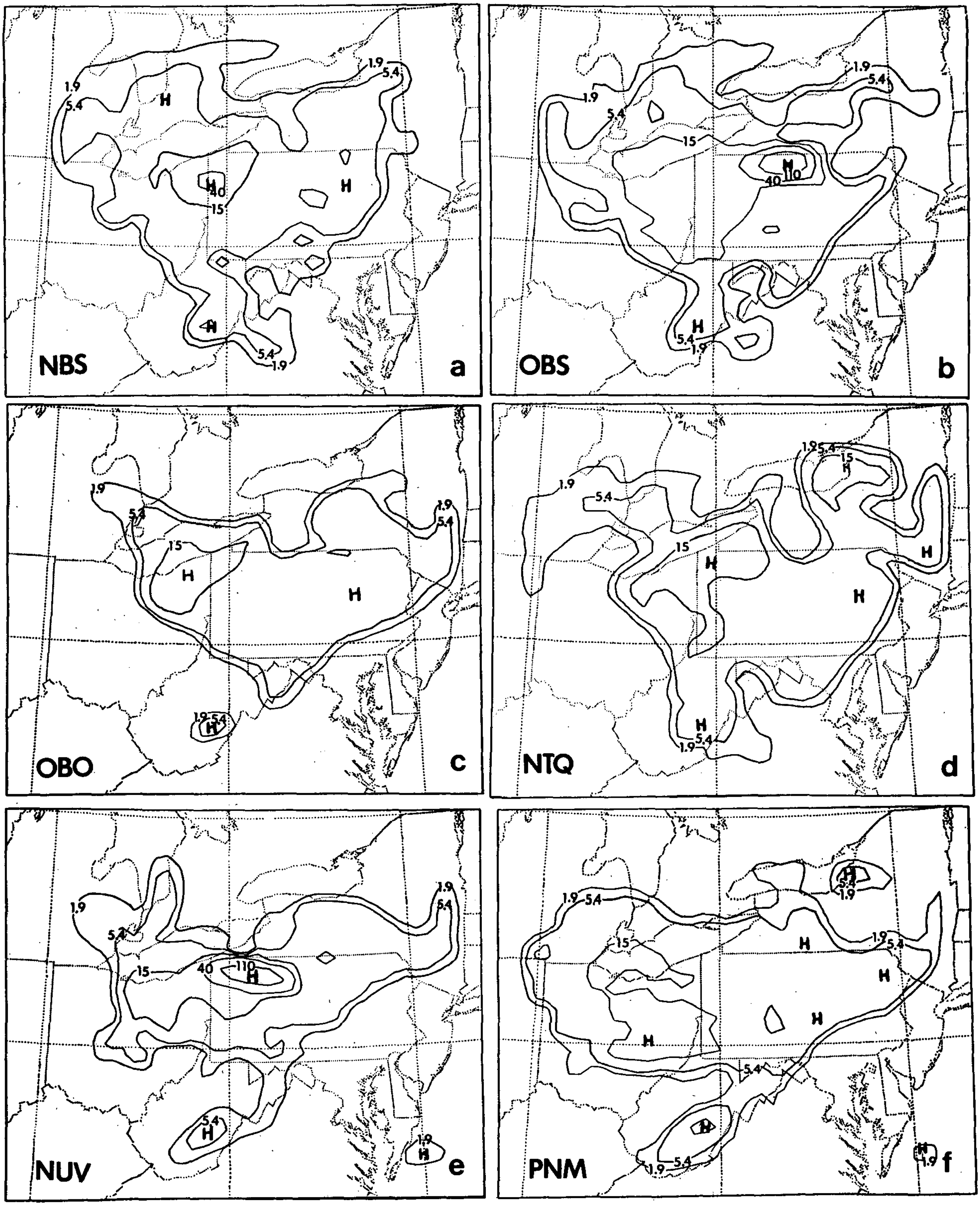

FIG. 9. Predicted 12 h accumulated rainfall (mm) for Exps. (a) NBS, (b) OBS, (c) OBO, (d) NTQ, (e) NUV, and (f) PNM. Relative maxima are indicated by H's.

d. Twelve h accumulated rainfall

Figure 9 shows the 12-h accumulated rainfall for each of the sensitivity experiments. The control simulation rainfall was shown in Fig. 2f and the observed rainfall is presented in Fig. 10.[2] For each of the experiments, the general shape of the precipitation area resembles the observed area. Note also that in each case there is a well-defined precipitation maximum over eastern Ohio/western Pennsylvania and the suggestion of a much weaker maximum in the northeastern portion of the rainfall area. This same relative distribution of the precipitation is also evident in the observed rainfall pattern. The similarities in the shape and distribution of the rainfall are further evidence that the meso-α-scale environment contains some type of signal that determines the general evolution of events. Moreover, in this regard, it is very interesting that what seems like rather large differences in the meso-β-scale pressure field do not have much effect on the general rainfall pattern.

While the general precipitation patterns are similar to the observed, the areas tend to be too large in most cases and there are significant differences in the meso-β-scale structure. The most important of these differences, from a practical standpoint, is the magnitude and location of the extremely heavy rain. Maximum amounts vary from about 25 mm in the experiments where a major mesolow does not develop to over 100 mm in the simulations where the mesolow appears. Thus, predictability of the *general* rainfall pattern seems to be reasonably stable, but certain important meso-β-scale rainfall features are very sensitive to the initial mesoscale thermodynamic fields (e.g., to the moisture profile in the Lake Erie sounding, as discussed previously). The significant change in precipitation that results from slightly altering a moisture profile is similar to results from Perkey's (1976; 1980) experimental forecasts. He noted that without any increase in total moisture content, a threefold increase in rainfall can be generated just by perturbing the initial moisture field.

It is worth pointing out that the additional wind information from Bosart's soundings did not have much effect on the precipitation pattern and amounts. In fact, in an additional experiment (not shown) where all of Bosart's wind information was excluded, but the Flint wind sounding was included, the precipitation pattern was virtually the same as in the control simulation. Such insignificant model sensitivity to detailed mesoscale wind information has also been found in a numerical study of dry sea-breeze circulations (see Carpenter and Lowther, 1982). On the other hand, when the Flint sounding was omitted and the meso-α-scale, low-level jet shifted southwestward, there was a corresponding shift in the region of significant precipitation.

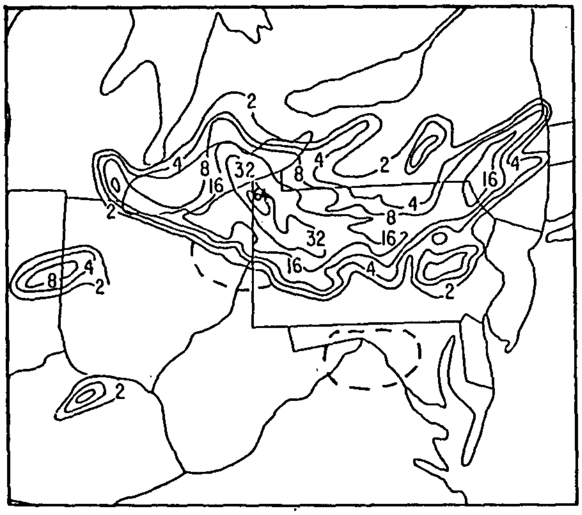

FIG. 10. Observed 12 h rainfall (mm) for the period 1200 GMT 19 July to 0000 GMT 20 July 1977 (from Bosart and Sanders, 1981). Dashed line indicates area of convection evident from satellite image and radar echoes during 2100–0000 GMT 19 July (see Hoxit et al., 1978).

5. Summary and concluding remarks

Six numerical sensitivity experiments on the Johnstown flood event of 1977 have been described. The experiments were designed to 1) test the sensitivity of a numerical simulation of MCSs to different types of initial conditions; 2) examine the need for an observing system that will resolve mesoscale features; and 3) determine which meteorological variables need to be most carefully considered in observing-system design and preprocessing analysis. Based on the results of these experiments, the following conclusions seem warranted:

- Improved observational capabilities are likely to have an important impact on the successful prediction of the timing and location of meso-β-scale convective weather systems if mesoscale features can be resolved. Without the initial mesoscale features, the numerical simulations only reproduced certain components of the MCSs and this led to significant changes in the results by the end of the 12 h period.
- The resolution of the moisture field significantly affects the prediction of the evolution of the convective weather systems. Correspondingly, the meso-β scale distribution of precipitation is also significantly affected, particularly the locations of the area of heavy rain. The importance of the moisture field stems from the sensitivity of meso-β-scale vortex development to

---

[2] While no precipitation is indicated over West Virginia and Maryland in Fig. 10, satellite and radar analyses indicate that rain did occur in this region (see Hoxit et al., 1978; Zhang and Fritsch, 1986). Also, Hoxit et al. indicated a 100 mm precipitation maximum over northwestern Pennsylvania.

the low-level and midlevel moisture content (in addition to favorable larger-scale forcing). Whether or not vortex genesis occurs has a large impact on the location of *heavy* precipitation and the evolution of other events. Mesovortices have been noted to develop relatively frequently in conjunction with MCCs (Johnston, 1981). Thus, successful prediction of the development and evolution of MCSs may hinge upon a model's ability to determine whether or not a vortex develops, and if it does, does it occur at the right time and location?

- Procedures to account for the effects of convective systems that are in progress at the time of initialization can make significant contributions to the prediction of the evolution of the meteorological events and to the improvement of the quantitative precipitation forecasts. In particular, in weak-gradient summertime situations, the MCSs can severely alter their near environment within a short time period by producing strong mesoscale circulations, thermal boundaries, moist adiabatic stratifications, etc. Thus, the subsequent evolution of convection can be affected. Salmon (1985) developed a procedure (from another viewpoint) to include the condensational heating that is in progress at the initial model time. Her results strongly support the above notion. Moreover, from an operational forecaster's viewpoint, Hales (1979) found that a subjective assessment of initial conditions is necessary in order to improve operational model forecasts when satellite imagery indicates a significant area of deep clouds over a data-void region.
- *For summertime situations in which the large-scale gradients are weak,* the detailed temperature and moisture fields appear to be more important than the detailed wind fields in determining the development and evolution of deep convection. This conclusion essentially agrees with dry sea-breeze experiments by Carpenter and Lowther (1982) and also with geostrophic adjustment theory, although the forcing resulting from the MCSs in the present case was involved in the model adjustment processes. The dominant role of the thermodynamic fields may be due to the fact that the distribution of temperature and moisture determines the distribution of available buoyant energy and this is usually relatively large in situations where MCSs develop (see Maddox, 1980; 1983). However, this dominance does not imply that efforts to obtain detailed wind fields are unnecessary since information contained in the detailed wind fields may possibly be transferred to the mass fields as a part of preprocessing the initial data. In fact, accurate determination of convergence and divergence is especially important for determining where the model convection should occur during the initial stage of a model integration. In addition, if the mesoscale wind field significantly departs from the mass field, the wind can modify the thermodynamic environment in such a way as to affect the timing and location of the deep convection.
- Incorporation of dense surface observations into the initial conditions can be very important in improving forecasts of meso-β-scale structures, such as moist (dry) tongues, thermal boundaries, and, in particular, the pressure distribution.
- Poor resolution of *meso-α-scale* gradients can significantly alter the predicted evolution of *meso-β-scale* features and the location of heavy rain.
- Poor resolution of the wind field such that the magnitude and gradients in wind speed are underestimated tends to reduce the degree of mesoscale organization and modify thermodynamic structure for the occurrence of the deep convection.
- *The large (meso-α) scale environment appears to contain some type of signal such that the general evolution of events is similar, even when the initial mesoscale structure and the simulated meso-β scale-evolution of events are significantly different.*

It is important to point out that the above conclusions may be "case dependent." Whether they are valid in a wide range of circumstances needs to be tested with additional numerical studies on other mesoscale meteorological events. In summary, it appears that for an environment in which the synoptic or meso-α-scale dynamics (e.g., thermal and/or vorticity advection, and/or frontal lifting) are weak and the thermodynamics (buoyant energy and/or latent heating) are strong, inclusion of mesoscale details such as moist (dry) tongues, thermal boundaries, pressure perturbations, etc., are essential for the successful prediction of the evolution of MCSs and their precipitation distribution. The Johnstown flood case is typical of summertime events with weak dynamics and strong thermodynamics. These conditions are also likely to be present during the development of many MCCs in the summer months in the United States (Maddox, 1980; 1983). Thus, significant improvement (from a modeling standpoint) in forecasts of the timing and location of the meso-β-scale structure and evolution of MCSs and, in particular, heavy rain, may have to wait until mesoscale features can be routinely incorporated into the initial conditions of operational models. On the other hand, it is very encouraging that the large (meso-α)-scale initial conditions still appear to contain sufficiently strong signals to determine the *general* structure and evolution of mesoscale events.

Acknowledgments. This work was supported by NSF Grants ATM-8218208 and ATM-8113223, USAF AFOSR-83-0064, and NOAA Cooperative Agreement NA82AA-H-00027. The authors are grateful to Drs. L. Bosart and J. Molinari for providing the subjectively analyzed data set for the initial conditions and to Ms. Sue Frandsen for skillfully preparing the manuscript. The computations were performed at the National Center for Atmospheric Science which is sponsored by the National Science Foundation.

REFERENCES

Anthes, R. A., and T. T. Warner, 1978: Development of hydrodynamic models suitable for air pollution and other mesometeorological studies. *Mon. Wea. Rev.*, **106**, 1045–1078.

——, and D. Keyser, 1979: Tests of a fine-mesh model over Europe and the United States. *Mon. Wea. Rev.*, **107**, 963–984.

——, E.-Y. Hsie, D. Keyser and Y.-H. Kuo, 1981: Impact of data and initialization procedures on variations of vertical motion and precipitation in mesoscale models. *Proc. IAMAP Symp.*, Hamburg, 245–257. [ESA Sp-165, 8–10, Rue Mario-Nikis, 75738 Paris, 15, France.]

Bosart, L. F., and F. Sanders, 1981: The Johnstown flood of July 1977: A long-lived convective storm. *J. Atmos. Sci.*, **38**, 1616–1642.

Carpenter, K. M., and L. R. Lowther, 1982: An experiment on the initial conditions for a mesoscale forecast. *Quart. J. Roy. Meteor. Soc.*, **108**, 643–660.

Chang, C. B., D. J. Perkey and C. W. Kreitzberg, 1984: Impact of initial wind field on the forecast of a severe storm environment. *Preprints, Tenth Conf. on Weather Forecasting and Analysis*, 513–520. [Available from Amer. Meteor. Soc., 45 Beacon St., Boston, MA 02108.]

Charba, J. P., and W. H. Klein, 1980: Skill in precipitation forecasting in the National Weather Service. *Bull. Amer. Meteor. Soc.*, **61**, 1546–1555.

Fawcett, E. B., 1977: Current capabilities in prediction at the National Weather Service's National Meteorological Center. *Bull. Amer. Meteor. Soc.*, **58**, 143–149.

Fritsch, J. M., and C. F. Chappell, 1980: Numerical prediction of convectively driven mesoscale pressure systems. Part I: Convective parameterization. *J. Atmos. Sci.*, **37**, 1722–1733.

——, and ——, 1981: Preliminary numerical tests of the modification of mesoscale convective systems. *J. Appl. Meteor.*, **20**, 910–921.

Gage, K. S., and J. L. Green, 1982: A technique for determining the temperature profile from VHF radar observations. *J. Appl. Meteor.*, **21**, 1146–1149.

Glahn, H. R., 1985: Yes, precipitation forecasts have improved. *Bull. Amer. Meteor. Soc.*, **66**, 820–830.

Hales, J. E., Jr., 1979: A subjective assessment of model initial conditions using satellite imagery. *Bull. Amer. Meteor. Soc.*, **60**, 206–211.

Hogg, D. C., M. T. Decker, F. O. Guiraud, K. B. Earnshaw, D. A. Merritt, K. P. Moran, W. B. Sweezy, R. G. Strauch, E. R. Westwater and C. G. Little, 1983: An automatic profiler of the temperature, wind, and humidity in the troposphere. *J. Climate Appl. Meteor.*, **22**, 807–831.

Hoxit, L. R., R. A. Maddox, C. F. Chappell, F. L. Zuckerberg, H. M. Mogil, I. Jones, D. R. Greene, R. E. Saffle and R. A. Scofield, 1978: Meteorological analysis of the Johnstown, Pennsylvania, flash flood, 19–20 July 1977. *NOAA Tech. Rep. ERL 401-APCL43*, 71 pp. [Available from Superintendent of Documents, U.S. Government Printing Office, Washington, D.C. 20402. Stock No. 003-017-00445-17.]

Johnston, E. C., 1981: Mesoscale vorticity centers induced by mesoscale convective complexes. M.S. thesis, Dept. of Meteorology, University of Wisconsin, 54 pp.

Kelly, G. A. M., G. A. Mills and W. L. Smith, 1978: Impact of Nimbus-6 temperature soundings on Australian region forecasts. *Bull. Amer. Meteor. Soc.*, **59**, 393–405.

Maddox, R. A., 1980: Mesoscale convective complexes. *Bull. Amer. Meteor. Soc.*, **61**, 1374–1387.

——, 1983: Large-scale meteorological conditions associated with midlatitude, mesoscale convective complexes. *Mon. Wea. Rev.*, **111**, 1475–1493.

Perkey, D. J., 1976: A description and preliminary results from a fine-mesh model for forecasting quantitative precipitation. *Mon. Wea. Rev.*, **104**, 1513–1526.

——, 1980: Impact of moisture on regional-scale numerical model simulations. *Atmospheric water vapor.* A. Deepak, T. D. Wilkerson and L. H. Ruhnke, Eds., Academic Press, 513–526.

——, and C. W. Kreitzberg, 1976: A time-dependent lateral boundary scheme for limited-area primitive equation models. *Mon. Wea. Rev.*, **104**, 744–755.

Salmon, E. M., 1985: Short-term numerical precipitation forecasts based on an initialization using a diagnosed divergent-wind component. M.S. thesis, Dept. of Meteorology, Pennsylvania State University, 122 pp.

Shuman, F. G., 1978: Numerical weather prediction. *Bull. Amer. Meteor. Soc.*, **59**, 5–17.

Westwater, E. R., Z.-H. Wang, N. C. Grody and L. M. McMillin, 1985: Remote sensing of temperature profiles from a combination of observations from the satellite-based microwave sounding unit and the ground-based profiler. *J. Atmos. Oceanic Technol.*, **2**, 97–109.

Zhang, D.-L., 1985: Nested-grid simulation of the meso-β scale structure and evolution of the Johnstown flood of July 1977. Ph.D. dissertation, Pennsylvania State University, 270 pp.

——, and R. A. Anthes, 1982: A high-resolution model of the planetary boundary layer-sensitivity tests and comparisons with SESAME-79 data. *J. Appl. Meteor.*, **21**, 1594–1609.

——, and J. M. Fritsch, 1985: Numerical simulation of a meso-β scale warm-core vortex over land. *Preprints, 14th Conf. on Severe Local Storms*, J29–32. [Available from Amer. Meteor. Soc., 45 Beacon St., Boston, MA 02108.]

——, and ——, 1986: Numerical simulation of the meso-β scale structure and evolution of the 1977 Johnstown flood. Part I: Model description and verification. *J. Atmos. Sci.*, **43**, 1913–1943.

——, H.-R. Chang, N. L. Seaman, T. T. Warner and J. M. Fritsch, 1986: A two-way-interactive, nesting procedure with variable terrain resolution. *Mon. Wea. Rev.*, **114**, 1330–1339.